Evaluation and Optimization of a Force Field for Crystalline Forms of Mannitol and Sorbitol

ARTICLE *in* THE JOURNAL OF PHYSICAL CHEMISTRY B · DECEMBER 2009

Impact Factor: 3.3 · DOI: 10.1021/jp9052665 · Source: PubMed

Evaluation and Optimization of a Force Field for Crystalline Forms of Mannitol and Sorbitol

H. de Waard,[†] A. Amani,[‡,§] J. Kendrick,[‡] W. L. J. Hinrichs,[†] H. W. Frijlink,[†] and J. Anwar*[,‡]

Department of Pharmaceutical Technology and Biopharmacy, University of Groningen, Antonius Deusinglaan 1, 9713 AV Groningen, The Netherlands, Computational Biophysics Laboratory, Institute of Pharmaceutical Innovation, University of Bradford, West Yorkshire, BD7 1DP, United Kingdom, and Department of Medical Nanotechnology, School of Advanced Medical Technologies, Tehran University of Medical Sciences, Tehran, Iran

Received: June 4, 2009; Revised Manuscript Received: October 30, 2009

Two force fields, the GROMOS53A5/53A6 (united atom) and the AMBER95 (all atom) parameter sets, coupled with partial atomic charges derived from quantum mechanical calculations were evaluated for their ability to reproduce the known crystalline forms of the polyols mannitol and sorbitol. The force fields were evaluated using molecular dynamics simulations at 10 K (which is akin to potential energy minimization) with the simulation cell lengths and angles free to evolve. Both force fields performed relatively poorly, not being able to simultaneously reproduce all of the crystal structures within a 5% deviation level. The parameter sets were then systematically optimized using sensitivity analysis, and a revised AMBER95 set was found to reproduce the crystal structures with less than 5% deviation from experiment. The stability of the various crystalline forms for each of the parameter sets (original and revised) was then assessed in extended MD simulations at 298 K and 1 bar covering 1 ns simulation time. The AMBER95 parameter sets (original and revised) were found to be effective in reproducing the crystal structures in these more stringent tests. Remarkably, the performance of the original AMBER95 parameter set was found to be slightly better than that of the revised set in these simulations at 298 K. The results of this study suggest that, whenever feasible, one should include molecular simulations at elevated temperatures when optimizing parameters.

1. Introduction

Polyols, or sugar alcohols, such as erythritol, isomalt, lactitol, sorbitol, mannitol, maltitol, and xylitol, are important components in many food, confectionery, and pharmaceutical products. Within the food industry, polyols are commonly used as sugar replacers, since they have a lower caloric content than sugars and they do not contribute to tooth decay. Additionally, due to the high negative heat of solution, inclusion of polyols like mannitol and sorbitol gives a cooling sensation in products like, for example, chewing gum.[1] The use of polyols in pharmaceuticals is widespread.[2] Mannitol, for example, is employed as a diluent (to increase the overall mass of a tablet containing a potent drug) and as a direct-compression aid in tablet formulations,[3,4] in wet granulation, as a plasticizer in soft gelatin capsules, as a carrier in dry powder inhalers, and as a bulking agent or for its possible lyoprotectant effect in freeze-dried products.[5–8] In addition to these applications, it can be administered parenterally for its therapeutic role in reducing the intracranial pressure or for its function as an osmotic diuretic. Recently, we described the use of mannitol for stabilizing nanocrystals of pharmaceutically active substances.[9,10] In this application, mannitol forms the matrix into which the drug nanocrystals are embedded. Nanocrystals of poorly water-soluble pharmaceuticals, because of their immense surface area, promise to significantly enhance the bioavailability of poorly soluble compounds.[11,12] Sorbitol (also called glucitol) can be employed as an alternative to mannitol, but because of its rather different physical properties it also has other niche applications that include its use as a humectant in oral solutions, in oral suspensions, in toothpastes, and in dermal products.[2] A notable feature of many of the above applications is that the polyols are exploited for their solid state properties.

Mannitol and sorbitol are stereoisomers of hexan-1,2,3,4,5,6-hexol ($HO-CH_2-CHOH-CHOH-CHOH-CHOH-CH_2OH$) (see Figure 1) and are known (or claimed) to exist in numerous crystalline polymorphs. Although the two chemical structures are similar, their physical properties differ markedly. For example, the melting points of the mannitol polymorphs vary over the range 155−166 °C, while the corresponding range for sorbitol is 93−112 °C. Furthermore, mannitol has a lower affinity for moisture, compared with the highly hygroscopic sorbitol. Mannitol is claimed to exist in at least eight polymorphic forms. Burger et al.[13] have extensively reviewed these claims and have reduced the number of anhydrous polymorphs to three: α-, β-, and δ-mannitol. The β-polymorph, which is the main commercially available product, is the thermodynamically stable form under ambient conditions. The δ-polymorph shows considerable kinetic stability, since it has been observed to show no transformation when subjected to mechanical stress or on storage (dry) for more than 5 years at 25 °C.[13] For sorbitol, even more polymorphs have been identified at room temperature: five anhydrous (A-, B-, Δ-, E-, and Γ-sorbitol) and two hydrated (sorbitol hydrate I and II) crystal forms. However, the structures of only three of the anhydrous forms, namely, A-sorbitol,[14] B-sorbitol,[15] and Γ-sorbitol,[16] have been determined. A key structural variation between the various polymorphic forms of both sorbitol and mannitol tends to be in the

* Corresponding author. E-mail: j.anwar@bradford.ac.uk.
[†] University of Groningen.
[‡] University of Bradford.
[§] Tehran University of Medical Sciences.

10.1021/jp9052665
Published on Web 12/15/2009

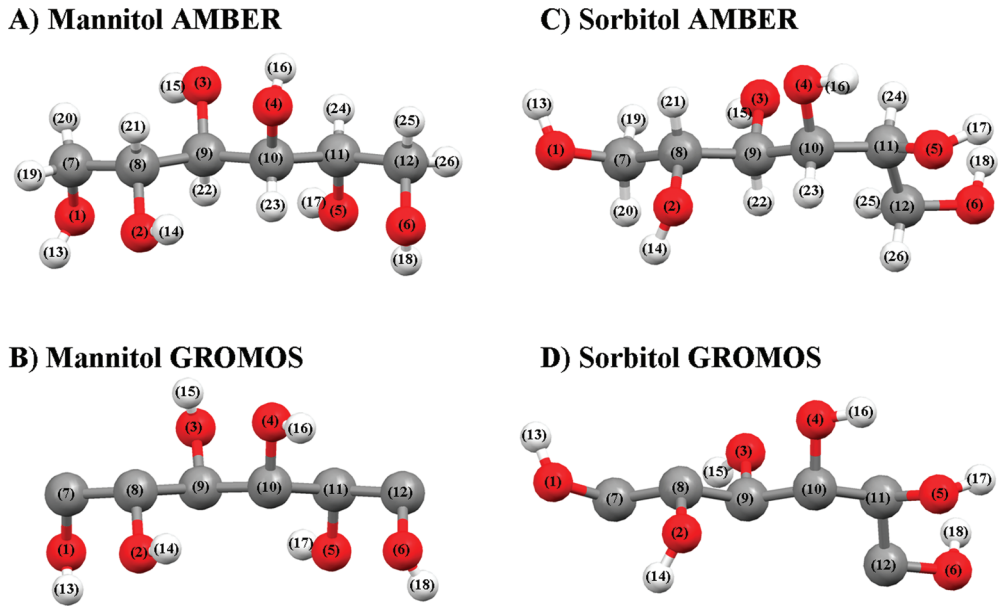

Figure 1. Molecular structures of mannitol and sorbitol showing indices of atoms for mapping force field atom types: (A) mannitol (AMBER95 force field); (B) mannitol (GROMOS53A5/53A6 force field); (C) sorbitol (AMBER95 force field); (D) sorbitol (GROMOS53A5/53A6 force field).

hydrogen bonding, more specifically in terms of the choice of whether a particular OH-group engages intra- or intermolecularly.[14–18]

In addressing fundamental and technological issues in materials behavior and function and solid state chemistry, molecular simulations are increasingly adding value to experimental studies. Molecular simulations can provide molecular-level insights and enable estimation/prediction of thermodynamic quantities.[19–21] The reliability of these simulations depends on the quality of the input parameters, namely, the force field that characterizes the interaction forces between the atoms. Despite the immense utility of both mannitol and sorbitol and the need to understand the molecular interactions of these materials with drug substances (including therapeutic peptides and proteins) and other formulation excipients, there are hardly any molecular simulation studies involving mannitol and sorbitol, particularly in the solid state. A possible obstacle is likely to be the reliability of the currently available force field parameters which have neither been tested nor optimized to reproduce the various crystalline forms of both sorbitol and mannitol. Indeed, the accuracy of force field parameters is at the heart of our ability (or inability, depending on one's perspective) to predict crystalline structures from first principles using intermolecular potentials.[22]

In this study, we have tested two force fields, GROMOS53A5/53A6 (united atom)[23] and AMBER95 (all-atom),[24] for their ability to reproduce the crystal structures of the known polymorphs of both mannitol and sorbitol. Both force fields in their original form were found to perform poorly in reproducing all of the experimental crystal structures in low temperature (10 K) molecular dynamics simulations, which is akin to potential energy minimization. We attempted to optimize the force fields, with the critical parameters being determined by sensitivity analysis. We were able to improve on the AMBER parameters so as to reproduce the various structures to less than 5% deviation in the cell parameters but were unable to make any progress with the GROMOS parameters. Remarkably, on validation of the parameters in molecular dynamics simulations at room temperature, the original AMBER parameters were found to perform slightly better than the optimized AMBER parameters (optimized at 10 K). The study illustrates the challenges of optimizing potential parameters for systems where the potential energy surface for the molecular interactions is characterized by many potential energy minima of similar depths, as typified by the various crystalline forms of mannitol and sorbitol in which a particular OH group can engage in intra- and intermolecular hydrogen bonding simply by rotation about a bond. The study suggests that optimization of potential parameters for crystalline phases should also include molecular simulations at the relevant temperatures and pressures and not only 0 K potential energy minimization, which should now be feasible given the increase in available computational power and the highly parallel nature of the problem.

2. Methods

2.1. Determination of Partial Charges. A single set of derived charges was employed for both force fields that were evaluated. To calculate the atomic partial charges, three conformationally distinct molecules each of both mannitol and sorbitol were taken from the crystal structures (DMANTL08, DMANTL09, and DMANTL10 for α-, β-, and δ-mannitol, respectively,[25] and GLUCIT01,[14] GLUCIT02,[15] and GLUCIT03[16] for A-, B-, and Γ-sorbitol respectively) and optimized using the General Atomic and Molecular Electronics Structure System-UK (GAMESS-UK) ab initio package[26] using the hybrid B3LYP density functional method with a 6-31G* basis set. The partial charges were calculated from the final electron densities using the electrostatic potential fitting method.[27] The fitting produced a single set of charges that provided the best fit to the electrostatic potential for all six molecular structures simultaneously, thus encapsulating any variation in the partial charges due to molecular conformation.

2.2. Evaluation of Force Fields. The two force fields, the GROMOS53A5/53A6 (united atom)[23] and AMBER95[24] parameter sets (see Tables 1 and 2), were evaluated by means of molecular dynamics simulations at 10 K for their ability to reproduce the known crystal structures of the anhydrous polymorphs of both mannitol and sorbitol. At this low simulation temperature, the procedure is essentially equivalent to potential energy minimization, and hence very much in the same spirit as the conventional approach for testing force fields. The

TABLE 1: Mapping of the GROMOS53A5/53A6[23] Parameters to the Mannitol and Sorbitol Molecules

Nonbonded Terms			
atom[a]	atom types	A^b (kJ mol^{-1} Å^{12})	B^b (kJ mol^{-1} Å^6)
1−6	OA	1210000[c]/1505529[d]	2093.98
7, 12	CH_2	33965584	7468.42
8−11	CH_1	97022500	6068.41
13−18	HO	0	0

$$U_{\text{vdw}}(r_{ij}) = \frac{A_{ij}}{r_{ij}^{12}} - \frac{B_{ij}}{r_{ij}^{6}}$$

Bonded Terms		
bonds	length (Å)	
OA−CH_2	1.43	
OA−CH_1	1.43	
OA−H	1.00	
CH_2−CH1	1.53	
CH_1−CH_1	1.53	
angles	k_θ (kJ mol^{-1})	θ_0 (deg)
OA−CH_2−CH_1	520	109.5
OA−CH_1−CH_2	520	109.5
OA−CH_1−CH_1	520	109.5
CH_2− OA−H	450	109.5
CH_2−CH_1−OA	520	109.5
CH_2−CH_1−CH_1	520	109.5
CH_1−OA−H	450	109.5
CH_1−CH_1−OA	520	109.5
CH_1−CH_1−CH_1	520	109.5

$$U_{\text{angles}}(\theta) = \frac{k_\theta}{2}(\cos\theta - \cos\theta_0)^2$$

dihedrals[e]	k_ϕ (kJ mol^{-1})	δ	m
X−CH_n− CH_n −X	5.92	0	3
X−CH_n− OA −X	1.26	0	3

$$U_{\text{dihedrals}}(\phi) = k_\phi[1 + \cos(m\phi - \delta)]$$

[a] Atom indices correspond to those given in Figure 1.

[b] $A_{ij} = \sqrt{A_{ii} \cdot A_{jj}}; \qquad B_{ij} = \sqrt{B_{ii} \cdot B_{jj}}$

[c] Used for OA−CH_2, OA−CH_1, and OA−H nonbonded interactions. [d] Used for OA−OA nonbonded interactions. [e] For any bond between two atoms (j and k), only one set of atoms (i, j, k, l) is chosen that define the dihedral angle.

dynamics simulations were carried out using the DL_POLY 2.18 package[28] in a NσT ensemble with the external pressure set to 1 bar and temperature and pressure coupling constants of 0.1 and 1.0 ps, respectively.[29] The NσT ensemble allows cell angles and cell lengths to change independently as a result of stress variations within the cell. The only restriction on the molecule internal degrees of freedom was that the bonds were constrained using the SHAKE algorithm. The electrostatic interactions were calculated using Ewald summation at a precision of 10^{-5}. The cutoffs for the van der Waals interactions and the real space Ewald were both 1.2 nm. The time step was 0.002 ps, and the total simulation time was 50 ps. All simulations converged relatively rapidly, and the cell angles and cell lengths were averaged over the final 30 ps.

TABLE 2: Mapping of the AMBER95[24] Parameters to the Mannitol and Sorbitol Molecule

Nonbonded Terms			
atom[a]	atom types	ε^a (kcal mol^{-1})	σ^a (Å)
1−6	OH	0.2104	1.5332
7−12	CT	0.1094	1.6998
13−18	HO	0.0000	0.0000
19−26	H1	0.0157	1.2357

$$U_{\text{LJ}}(r_{ij}) = 4\varepsilon_{ij}\left[\left(\frac{\sigma_{ij}}{r_{ij}}\right)^{12} - \left(\frac{\sigma_{ij}}{r_{ij}}\right)^{6}\right]$$

Bonded Terms		
bonds	length (Å)	
OA−CT	1.410	
OA−HO	0.960	
CT−CT	1.526	
CT−H1	1.090	
angles	k_θ/2 (kcal mol^{-1})	θ_0 (deg)
OA−CT−CT	50.0	109.5
OA−CT−H1	50.0	109.5
CT−OA−HO	55.0	108.5
CT−CT−OA	50.0	109.5
CT−CT−CT	40.0	109.5
CT−CT−H1	50.0	109.5
H1−CT−H1	35.0	109.5

$$U_{\text{angles}}(\theta) = \frac{k_\theta}{2}(\theta - \theta_0)^2$$

dihedrals	V_n/2 (kcal mol^{-1})	δ	m
X−CT−CT−X	0.156	0.0	3
X−CT−OH−X	0.167	0.0	3

$$U_{\text{dihedrals}}(\phi) = \frac{V_n}{2}[1 + \cos(m\phi - \delta)]$$

[a] Atom indices correspond to those given in Figure 1.

[b] $\varepsilon_{ij} = \sqrt{\varepsilon_{ii} \cdot \varepsilon_{jj}}; \qquad \sigma_{ij} = (\sigma_i + \sigma_j)/2$

2.3. Sensitivity Analysis and Optimization of Potential Parameters. Both the GROMOS and AMBER parameters failed to reproduce the various crystal structures of sorbitol and mannitol simultaneously. In view of this, we proceeded to optimize each of the parameter sets using an approach based on sensitivity analysis, which in an earlier study proved to be very effective in optimizing potential parameters for crystalline phases.[30] Sensitivity analysis involves investigating the significance of the effect of a small change in each of the parameters, and hence enables the identification of the critical parameters which can then be optimized. Here, we examined the effect of a 5% change in each of the potential parameters on the lattice parameters of the various phases in molecular dynamics simulations at 10 K, as detailed above. This enabled the identification of those parameters that had the most effect in reproducing the lattice parameters of the crystalline phases. The optimum values of the identified critical parameters were then identified by varying these parameters in isolation in small increments.

TABLE 3: Atomic Partial Charges Calculated from Electrostatic Potential Fitting[a]

AMBER force field			GROMOS force field		
atom	atom type	atomic partial charge (e)	atom	atom type	atomic partial charge (e)
1	OH	−0.582	1	OH	−0.582
2	OH	−0.590	2	OH	−0.590
3	OH	−0.590	3	OH	−0.590
4	OH	−0.590	4	OH	−0.590
5	OH	−0.590	5	OH	−0.590
6	OH	−0.582	6	OH	−0.582
7	CT	0.153	7	CH_2	0.211
8	CT	0.199	8	CH_1	0.217
9	CT	0.199	9	CH_1	0.217
10	CT	0.199	10	CH_1	0.217
11	CT	0.199	11	CH_1	0.217
12	CT	0.153	12	CH_2	0.211
13	HO	0.373	13	HO	0.373
14	HO	0.371	14	HO	0.371
15	HO	0.371	15	HO	0.371
16	HO	0.371	16	HO	0.371
17	HO	0.371	17	HO	0.371
18	HO	0.373	18	HO	0.373
19	H1	0.029			
20	H1	0.029			
21	H1	0.018			
22.	H1	0.018			
23	H1	0.018			
24	H1	0.018			
25	H1	0.029			
26	H1	0.029			

[a] The atom indices refer to the numbers given in Figure 1a and c for the AMBER force field and Figure 1b and d for the GROMOS force field.

The influence of the various van der Waals parameters for both force fields was determined by investigating the effect of a 5% increment in each of the homo-parameters (i.e., the A and B values for GROMOS and ε and σ values of the fully atomistic AMBER force field) in isolation. For this study, the hetero-parameters were calculated from the homo-parameters using standard mixing rules. A secondary study explored the effects of a 5% increment of the individual hetero-parameters, which of course makes the model more flexible but increases the parameter space considerably.

We also considered the force constants for the dihedral energy barriers as parameters that could benefit from optimization. This is unusual but necessary for the two molecules mannitol and sorbitol, since these force constants are expected to play an important role in determining the hydrogen-bonding interaction of the OH groups. One could attempt to calculate the specific torsional force constants for the two molecules from first principles by characterizing the potential energy surface for bond rotation about the dihedrals. However, such an approach still requires the removal of the electrostatic and van der Waals contributions of the 1−4 and above interaction from the potential energy (PE) surface, which may not be straightforward given that the van der Waals interactions themselves are not fixed and are the subject of optimization. In view of this, we proceeded with the original torsional force constants (which, in general, would have been determined from first principles and optimized, albeit for other simpler molecules) and considered them as parameters for optimization. Thus, the effect of 10, 20, and 40% variations in the force constants was examined for both the AMBER and GROMOS force fields. The van der Waals parameters were kept at their original values, while the torsional force constants were changed.

2.4. Validation: Molecular Dynamics Simulations of Mannitol and Sorbitol Crystals. The quality of the original and optimized parameter sets was tested in molecular dynamics simulations under ambient conditions. Thus, the stability of crystals of α-mannitol (8 × 4 × 2 unit cells; 256 molecules), β-mannitol (7 × 4 × 2 unit cells; 224 molecules), δ-mannitol (8 × 2 × 7 unit cells; 224 molecules), A-sorbitol (4 × 4 × 4 unit cells; 256 molecules), E-sorbitol (7 × 4 × 2 unit cells; 224 molecules), and Γ-sorbitol (2 × 2 × 8 unit cells; 384 molecules) was investigated in extended dynamics simulations performed in a NσT ensemble[29] at 298 K and 1 bar with a temperature and pressure coupling of 0.1 and 1.0 ps, respectively, using the same simulation parameters as specified in section 2.2 above. Each of the simulations accessed 1 ns simulation time.

3. Results and Analysis

3.1. Partial Charges. The partial atomic charges determined from simultaneously fitting the electrostatic potentials of the various molecular structures found in the polymorphs of anhydrous polymorphs of mannitol and sorbitol are shown in Table 3. The standard deviation of the electrostatic potential generated by this point charge model from the quantum-mechanical electrostatic potential was similar for all conformations and smaller than 0.009 (atomic units). The best fits to the electrostatic potential of fitting each molecule individually are all above 0.0077, while using a single charge assignment for all molecules gives values of less than 0.0084. For the united-atom force field, the charges on the aliphatic hydrogen were added to the charges of the carbons to which they are bonded, giving a total charge for the united atom.

3.2. Evaluation and Sensitivity Analysis of the GROMOS Force Field. For the GROMOS force field, the simulated crystal structures showed deviations in the cell lengths of up to 6% from the experimental values (Table S1, Supporting Information), with the *b*-axis of the β-polymorph of mannitol being the most problematic. In contrast, the cell angles of all crystals were found to deviate less than 0.5% from the experimental values.

TABLE 4: Optimization of the LJ σ-Parameter of the Hydroxyl Oxygen Atom (Atom Type OH) of the AMBER95 Force Field[a]

		α-mannitol			β-mannitol			δ-mannitol		
interaction	increase (%)	*a* (%)	*b* (%)	*c* (%)	*a* (%)	*b* (%)	*c* (%)	*a* (%)	*b* (%)	*c* (%)
OH−OH σ	0	−0.77	−1.78	−0.89	0.24	−0.15	−2.16	−8.37	2.17	−4.81
	2	0.55	−1.11	−0.90	1.87	0.43	−2.82	−6.75	2.74	−0.37
	3	1.26	−0.77	−0.89	2.72	0.74	−3.11	−5.91	2.96	−4.31
	4	1.97	−0.39	−0.88	3.55	1.14	−3.39	−5.34	−1.27	0.13
	5	2.68	−0.08	−0.87	4.38	1.43	−3.58	−4.35	−1.29	0.43
		A-sorbitol			E-sorbitol			Γ-sorbitol		
interaction	increase (%)	*a* (%)	*b* (%)	*c* (%)	*a* (%)	*b* (%)	*c* (%)	*a* (%)	*b* (%)	*c* (%)
OH−OH σ	0	−1.66	2.63	−2.57	−1.69	−0.55	0.27	0.25	0.03	−1.97
	2	−0.92	3.70	−1.82	−0.05	−0.37	0.78	0.65	−0.60	0.68
	3	−0.58	4.20	−1.33	0.71	−0.26	1.02	1.02	−0.87	1.05
	4	−0.19	4.75	−0.92	1.16	−0.22	1.25	1.13	−1.06	2.19
	5	0.12	5.24	−0.35	2.44	−0.16	1.44	1.33	−1.12	3.00

[a] The table gives the % deviation in the cell lengths of the simulated crystal structure from the experimental values as the LJ σ-parameter of the hydroxyl oxygen atoms is incremented.

Sensitivity analysis of the parameters revealed that the GROMOS force field was relatively robust with respect to the dihedral energy force constants, variations in which did not cause significant changes in the lattice parameters and neither induced the desired simultaneous overall improvement in the crystal lattices. Changes in the values for the dihedral energy barrier would therefore result in the improvement of some of the lattice parameters but compromise others. The *A* and *B* van der Waals homo-parameters for the atom (united) types CH_1 (aliphatic CH_1-group) and CH_2 (aliphatic CH_2-group) did not appear to affect the lattice parameters much. In contrast, the lattice parameters were highly sensitive to variations in both the *A* and *B* parameters for the atom type OA (the hydroxyl oxygen atoms), but the effect was never beneficial all around in reproducing all of the crystalline phases. Although the HO (hydroxyl hydrogen) van der Waals parameters in the original force field are set to zero, their influence was also examined. Variations in the HO *B*-parameter had a significant and positive effect toward reproducing the various crystalline lattices. This *B* parameter, however, represents the attractive component of the Lennard-Jones potential, and giving this a value while leaving the *A* parameter set at zero does not yield a proper LJ potential; hence, this course was rejected, being considered to be rather ad hoc. The analysis, however, clearly indicates that the hydroxyl descriptions are critical.

As our attempts to optimize the homo-parameters proved ineffective, we proceeded to investigate the sensitivity of the lattice parameters to variations in the individual hetero-parameters, which serve as a more flexible model. Modifying any of the interactions, with exception of the OH−HO (oxygen−hydrogen) interaction, did not result in any significant and/or overall beneficial change in the lattice parameters. Increasing the *A*-parameter (the repulsive component) of this interaction had a strong detrimental effect on all of the cell lengths (Table S2, Supporting Information). There was no option to reduce this parameter, since it is already set at zero (the lowest possible value with a physical basis) in the original force field. Therefore, it became apparent that there was no scope for optimizing the GROMOS force field for the various crystalline forms of mannitol and sorbitol.

3.3. Evaluation and Sensitivity Analysis of the AMBER95 Force Field. Attempts to reproduce the crystalline forms of mannitol and sorbitol using the AMBER95 force field revealed δ-mannitol as the problem phase, for which both the β-angle (by almost 12%) and the *a*-axis (by over 8%) were underestimated (Table S3, Supporting Information). Sensitivity analysis with respect to the dihedral energy force constants (Table S4, Supporting Information) showed that, while the lattice parameters were sensitive to variations in the force constants, any given change in the force constants did not consistently improve the crystal structure predictions.

With respect to the van der Waals homo-parameters, these too did not offer an option for optimization. It was found that changing the σ-parameter of the OH-atom had the strongest influence on the cell dimensions, with an increase of 5% of this value resulting in a strong improvement in the cell dimensions of δ-mannitol. However, at the same time, this variation was detrimental for the cell dimensions of the other structures, e.g., the β-angle of A-sorbitol.

Sensitivity analysis of the van der Waals hetero-parameters revealed that a variation in the σ-parameter of the OH−OH interaction could considerably improve the predicted lattice parameters, in particular eliminating the very large deviations (Table S5, Supporting Information). However, the effects of this parameter were not wholly beneficial, as some of the lattice deviations, which previously were low, were now larger. In view of this, the σ-parameter of the OH−OH interaction was optimized by investigating the effect of stepwise increments of 1% up to a maximum of 6%. The 4% increased value of the σ-parameter appeared to be optimal in characterizing all of the crystal forms of mannitol and sorbitol at 10 K (see Table 4). This increase in the σ-parameter represents a direct increase in the effective diameter of the hydroxyl oxygen atoms. For this optimal parameter set, the lattice energies (the potential energy/molecule of the crystal minus the intramolecular energy of a single molecule in vacuum) of the various forms of mannitol and sorbitol were −156.7, −161.6, and −153.6 kJ mol^{-1} for α-, β-, and δ-mannitol, respectively, and −165.6, −158.6, and −145.2 kJ mol^{-1} for A-, E-, and Γ-sorbitol, respectively. Unfortunately, there are no experimental data against which these values can be compared. While there does appear to be some correlation between the lattice energies and the melting points for mannitol (melting points 166, 166.5, and 150−158 °C for the α-, β-, and δ-forms, respectively), this is not the case for sorbitol for which the highest energy form Γ exhibits a markedly higher melting point of 98.7 °C compared with 88.1 °C for form A. Perhaps a more significant issue is that the lattice energies of the various forms of both mannitol and sorbitol are pretty similar, ranging from −145 to −166 kJ mol^{-1}, and yet the melting points of these two stereoisomers are markedly

TABLE 5: Deviation (%) in the Cell Lengths of the Simulated Crystal Structure from the Experimental Values for Various Polymorphic Forms of Mannitol and Sorbitol Averaged for the Latter Part of a Molecular Dynamics Simulation Trajectory at 298 K and 1 bar Pressure

	α-mannitol			β-mannitol			δ-mannitol		
	a (%)	*b* (%)	*c* (%)	*a* (%)	*b* (%)	*c* (%)	*a* (%)	*b* (%)	*c* (%)
GROMOS	10.71	6.01	−6.19	−0.76	8.79	1.18	10.50	−11.92	42.41
AMBER95	0.75	−0.04	−0.39	0.89	1.84	−1.21	−5.97	−1.09	0.70
AMBER optimized	3.80	1.40	−0.27	4.40	3.08	−1.87	−1.97	0.25	5.39
	A-sorbitol			E-sorbitol			Γ-sorbitol		
	a (%)	*b* (%)	*c* (%)	*a* (%)	*b* (%)	*c* (%)	*a* (%)	*b* (%)	*c* (%)
GROMOS	1.45	3.34	1.80	6.94	4.14	−2.18	6.88	−1.67	9.88
AMBER95	0.01	3.54	−1.34	1.26	0.56	−0.04	0.25	1.50	−0.31
AMBER optimized	1.70	5.74	0.35	5.70	1.41	0.22	1.67	1.92	2.97

TABLE 6: Root Mean Square Deviation (Å/atom) of the Atomic Coordinates of the Simulated Crystal Structure from the Experimental Values for Various Polymorphic Forms of Mannitol and Sorbitol Averaged for the Latter Part of a Molecular Dynamics Simulation Trajectory at 298 K and 1 bar Pressure

	α-mannitol	β-mannitol	δ-mannitol
GROMOS	0.299	0.201	0.239
AMBER95	0.265	0.187	0.218
AMBER optimized	0.505	0.231	0.330
	A-sorbitol	E-sorbitol	Γ-sorbitol
GROMOS	0.244	0.199	0.262
AMBER	0.373	0.300	0.541
AMBER optimized	0.721	0.268	0.417

different (mannitol, 150−167 °C; sorbitol, 88−99 °C). This suggests that the two stereoisomers accommodate thermal energy in markedly different ways; i.e., the respective entropy contribution to stability is significantly different.

3.4. Molecular Dynamics Simulation under Ambient Conditions. The quality of the optimized as well as the original AMBER parameters and original GROMOS parameters (which could not be optimized any further) was tested in extended molecular dynamics simulations at 298 K and 1 bar pressure, i.e., ambient conditions for each of the polymorphic forms of mannitol and sorbitol. In principle, only one of the polymorphic forms of each of the polyols is thermodynamically stable under ambient conditions, and an expectation may be that the other polymorphic forms would transform to the stable polymorphic form. While first-order phase transformations are indeed accessible in molecular dynamics simulations, these are largely restricted to systems with low activation energy barriers, which in the laboratory occur relatively rapidly.[31,32] Systems with strong hydrogen bonding tend to be relatively sluggish and require in excess of tens of nanoseconds of simulation time unless coerced using a biased potential method like metadynamics.[33] In view of these considerations, it was anticipated that the strongly hydrogen-bonded mannitol and sorbitol structures, which in the laboratory are kinetically stable for extended periods of time, were unlikely to undergo any transformation during the limited 1 ns simulations.

The results from the MD simulations, that is, the averaged lattice parameters, deviations in the lattice parameters from experiment, and the atom-based root mean squared deviations from the experimental structures, are presented in Tables 5 and 6. The data (Table 5) clearly reveal that the GROMOS parameters while being just outside the limit of respectability in the 10 K simulations are extremely poor in characterizing the various crystalline forms under ambient conditions. An extreme example is the marked deviation in the *c*-axis of δ-mannitol, which is overestimated by 42%. In contrast, the AMBER parameters, both original and optimized, fare much better (Table 5) and are able to reproduce the various crystalline structures reasonably well, within the limits of 6%. Remarkably, the original AMBER parameters (see Figure 2) result in a slightly better representation of the crystals than the optimized AMBER parameters (see Figure 3).

In general, the various polymorphs essentially retained their structures in the MD trajectories, other than the δ-polymorph of mannitol which showed some changes in its hydrogen-bonding interactions. The hydroxyl group (O3, H15) attached to carbon atom C9 appears to reveal a tendency to form an intramolecular H-bond while compromising an intermolecular H-bond interaction (see Figure 4).

4. Discussion

The objectives of the study were to identify a set of force field parameters that could simultaneously reproduce all known crystal structures of the various polymorphic forms of the

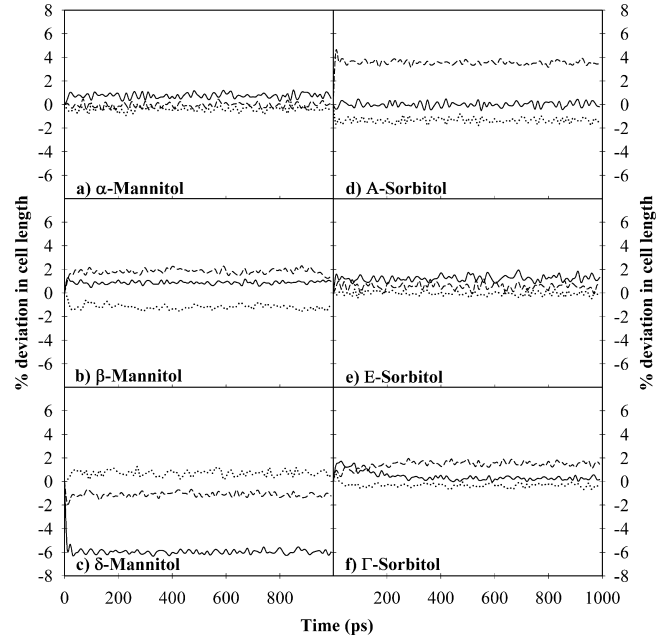

Figure 2. Deviation (%) in the cell dimensions between the simulated and experimental structure as a function of simulation time in a molecular dynamics simulation at 298 K and 1 bar using the original AMBER95 force field: (a) α-mannitol; (b) *β*-mannitol; (c) δ-mannitol; (d) A-sorbitol; (e) E-sorbitol; (f) Γ-sorbitol. (—) *a*-axis, (- - -) *b*-axis, and (•••) *c*-axis.

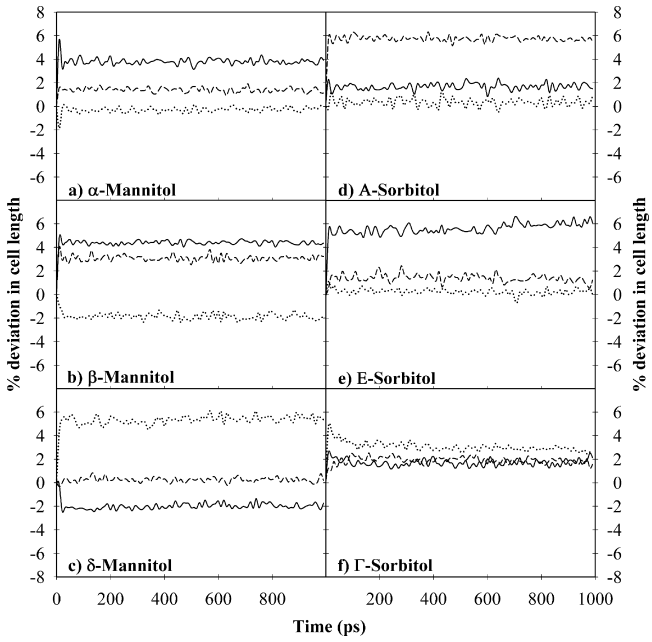

Figure 3. Deviation (%) in the cell dimensions between the simulated and experimental structure as a function of simulation time in a molecular dynamics simulation at 298 K and 1 bar using the optimized AMBER95 force field: (a) α-mannitol; (b) β-mannitol; (c) δ-mannitol; (d) A-sorbitol; (e) E-sorbitol; (f) Γ-sorbitol. (—) *a*-axis, (- - -) *b*-axis, and (•••) *c*-axis.

polyols, mannitol and sorbitol. We have tested two force fields, namely, the united atom GROMOS53A5/53A6 and the all atom AMBER95 parameter set, and then attempted to optimize them using sensitivity analysis. The worst case GROMOS performance was a 6% deviation in the cell parameters, just putting it outside the respectable 5% limit. The critical parameters were found to be the van der Waals parameters of the hydroxyl hydrogen atoms, an increase in which caused a larger deviation between the calculated and experimental cell parameters. For the GROMOS force field, these parameters are in fact set at zero; hence, there was little scope for any further optimization.

The AMBER95 parameter set appeared to perform even worse (maximum deviation for a lattice dimension >8%; for a cell angle >11%), with the critical parameters as identified by sensitivity analysis being the Lennard-Jones σ parameter of the OH−OH interaction and the X−CT−OH−X dihedral energy barrier. Optimizing the former enhanced the performance to a respectable level (worst cell deviation just over 5%), while the effect of varying the dihedral energy barrier was found to be inconsistent and irregular. We then proceeded to test the force fields, the original GROMOS and AMBER parameter sets, and the optimized AMBER parameters, in extended molecular dynamics simulations on mannitol and sorbitol crystals at 298 K and 1 bar. While the GROMOS parameter set resulted in almost complete instability in some of the structures, the AMBER95 parameters performed reasonably well. Remarkably, at 298 K, the original AMBER95 parameter set was a little better than the optimized parameters. The underlying issue of force fields that have been optimized using low temperature simulations performing badly at elevated temperatures is well understood. The optimization process is typically based on only a few crystal structures, limiting the number of molecular orientations that are sampled. At higher temperatures, the molecules sample an entire spectrum of orientational interactions of which the optimized parameters are uninformed. The puzzling aspect here is the converse observation of that of the AMBER parameters failing grossly in low temperature simulations while performing well at elevated temperatures. While the cause here is difficult to identify, it is probably pertinent to note that the AMBER nonbonded parameters were adopted from OPLS[34] and also derived using the OPLS philosophy of fitting parameters to simulations of liquid phases, i.e., simulations at elevated temperatures.[24] Despite the original AMBER95 parameters performing slightly better at 298 K, we propose the revised set (in which only the LJ σ-parameter of the OH−OH interaction is modified) as the definitive parameter set for future application, since it has better temperature dependence, i.e., from 0 K to ambient temperature.

It is legitimate to ask the question "why is it not possible to improve the accuracy of the force field parameters beyond that achieved?". The general response would be to highlight the difficulty of fitting a complex response surface (which is a function of the atomic coordinates in the crystal and their dependence as a function of time and temperature) with a limited set of parameters. There are however at least a couple more specific issues. First, a point charge description of the electrostatics is unable to describe either the conformational dependence of the charge distribution or the anisotropy of the charge−charge interactions; for greater accuracy, one needs to employ approaches like the atomic multipole model.[35] Most molecular simulation codes, however, only contain a point charge description, which restricts the use of atomic multipole-based force fields. A secondary issue is the anisotropy of the repulsion component of the van der Waals interaction,[36] though this is not expected to be a major problem for the atom types present in the polyols studied. Furthermore, in the present study, the atomic partial charges, which were determined from the electrostatic potential, were kept fixed and not subjected to systematic optimization. While this is the accepted philosophy, partial charges obtained from first principles can on occasion fare worse than fitted charges, as exemplified by the crystal structure prediction of glycine.[37] However, empirical optimiza-

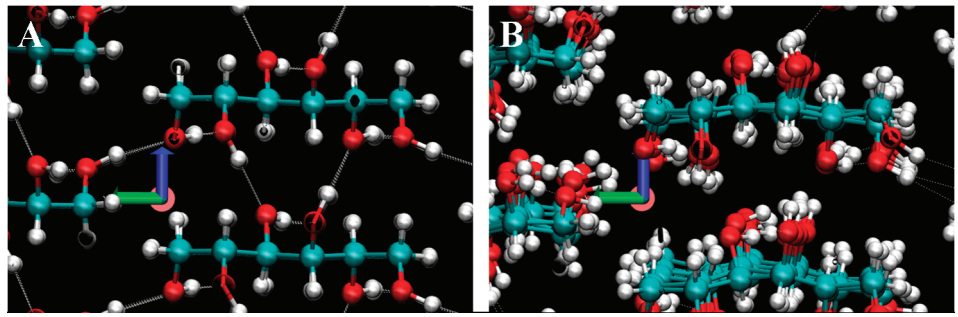

Figure 4. Comparison between the experimental structure (A) and a snapshot from the molecular dynamics trajectory under ambient conditions (B) for δ-mannitol showing the slight variation in the hydrogen-bonding interactions as a result of thermal energy.

tion of the charges could in principle yield a set of charges (which may or may not be intuitively sensible) that reproduce the structures extremely well in the testing protocol but completely fail in a real application. Furthermore, the partial charges are likely to be highly correlated with the van der Waals parameters, particularly the Lennard-Jones well-depth, ε, or equivalent. Because of these considerations, we thought it prudent not to optimize the charges.

While the study identifies a parameter set for future simulations of mannitol and sorbitol in the solid state, there are clearly some lessons to be learned with respect to the approaches commonly employed (and also employed here) for optimizing parameters for the solid state. The usual protocol in optimizing the parameters for the crystalline state is to attempt to reproduce the crystalline structure in a 0 K structural optimization, typically involving potential energy minimization with the lattice parameters, internal symmetry, and atomic coordinates being free to evolve. In the present study, we have employed low temperature (10 K) MD simulation with a fully flexible simulation cell, which essentially equates to potential energy minimization, since the thermal energy is very low, keeping the system close to the nearest local energy minima. We are, of course, interested in the molecular behavior at ambient temperature and pressure, and the optimized potential parameters are likely to be employed in molecular simulations under these conditions. Furthermore, the crystal structures to which the parameters are being fitted are certainly never determined at 0 K. Our results, which illustrate that a good performance of a force field at 10 K may not per se be reflected in an elevated temperature study, suggest that we should also include the stability assessment of the structures in molecular simulations (i.e., molecular dynamics or Monte Carlo simulation involving reasonable sampling or simulation time) at temperatures and pressures of interest in the optimization iteration cycle. Note that we cannot replace the potential energy minimization entirely by, for example, MD at ambient temperature, since it is very likely that some crystalline structures are likely to diverge from the experimental structure because they happen to be thermodynamically unstable under those conditions. In fact, contrary to what some might expect, obtaining such a result would confirm the accuracy of the employed force field.

Summarizing, we have tested and attempted to optimize the two force field parameter sets, GROMOS and AMBER95, to model the many crystalline forms of the polyols, mannitol and sorbitol. The AMBER95 parameter set with a modified LJ σ-parameter for the OH−OH interaction coupled with the derived atomic partial charges has been found capable of reproducing all of the known crystalline structures in MD simulations at 298 K for up to 1 ns. We intend now to employ this parameter set in exploring drug−polyol interfacial properties that underpin the stability of nanocrystals of pharmaceuticals embedded in polyol (crystalline and amorphous) matrices.

Acknowledgment. This research was performed within the framework of project T5-105 of the Dutch Top Institute Pharma.

Supporting Information Available: Tables showing evaluation and sensitivity analysis of the nonbonded homo-parameters and hetero-parameters of the GROMOS53A5/53A6 force field, evaluation and sensitivity analysis of the nonbonded homo-parameters of the AMBER95 force field, and sensitivity analysis of the dihedral energy force constants and the nonbonded hetero-parameters of the AMBER95 force field. This information is available free of charge via the Internet at http://pubs.acs.org.

References and Notes

(1) Bornet, F. R. J. *Am. J. Clin. Nutr.* **1994**, *59*, 763S.
(2) Rowe, R. C.; Sheskey, P. J.; Owen, S. C. *Handbook of pharmaceutical excipients*, 5th ed.; Pharmaceutical Press: London, 2005.
(3) Yoshinari, T.; Forbes, R. T.; York, P.; Kawashima, Y. *Int. J. Pharm.* **2003**, *258*, 121.
(4) Bolhuis, G. K.; Rexwinkel, E. G.; Zuurman, K. *Drug Dev. Ind. Pharm.* **2009**, *35*, 671.
(5) Johnson, R. E.; Kirchhoff, C. F.; Gaud, H. T. *J. Pharm. Sci.* **2002**, *91*, 914.
(6) Hawe, A.; Frieβ, W. *Eur. J. Pharm. Sci.* **2006**, *28*, 224.
(7) Liao, X.; Krishnamurthy, R.; Suryanarayanan, R. *Pharm. Res.* **2007**, *24*, 370.
(8) Pyne, A.; Chatterjee, K.; Suryanarayanan, R. *J. Pharm. Sci.* **2003**, *92*, 2272.
(9) de Waard, H.; Hinrichs, W. L. J.; Frijlink, H. W. *J. Controlled Release* **2008**, *128*, 179.
(10) de Waard, H.; Grasmeijer, N.; Hinrichs, W. L. J.; Eissens, A. C.; Pfaffenbach, P. P. F.; Frijlink, H. W. *Eur. J. Pharm. Sci.* **2009**, *38*, 224.
(11) Merisko-Liversidge, E.; Liversidge, G. G.; Cooper, E. R. *Eur. J. Pharm. Sci* **2003**, *18*, 113.
(12) Müller, R. H.; Peters, K. *Int. J. Pharm.* **1998**, *160*, 229.
(13) Burger, A.; Henck, J. O.; Hetz, S.; Rollinger, J. M.; Weissnicht, A. A.; Stottner, H. *J. Pharm. Sci.* **2000**, *89*, 457.
(14) Park, Y. J.; Jeffrey, G. A. *Acta Crystallogr.* **1971**, *B27*, 2393.
(15) Schouten, A.; Kanters, J. A.; Kroon, J.; Comini, S.; Looten, P.; Mathlouthi, M. *Carbohydr. Res.* **1998**, *312*, 131.
(16) Rukiah, M.; Lefebvre, J.; Hernandez, O.; Beek, W. v.; Serpellonid, M. *J. Appl. Crystallogr.* **2004**, *37*, 766.
(17) Kim, A. I.; Akers, M. J.; Nail, S. L. *J. Pharm. Sci.* **1998**, *87*, 931.
(18) Berman, H. M.; Jeffrey, G. A.; Rosenstein, R. D. *Acta Crystallogr.* **1968**, *B24*, 442.
(19) Catlow, C. R. A.; Ackermann, L.; Bell, R. G.; Corà, F.; Gay, C. D. H.; Nygren, M. A.; Pereira, J. C.; Sastre, G.; Slater, C. B.; Sinclair, P. E. *Faraday Discuss.* **1997**, *106*, 1.
(20) Frenkel, D.; Smit, B. *Understanding molecular simulations: From algorithms to applications*, 2nd ed.; Academic Press: San Diego, CA, 2002; Vol. 1.
(21) Chipot, C.; Pohorille, A. *Free energy calculations: Theory and applications in chemistry and biology*; Springer: Heidelberg, Germany, 2007; Vol. 86.
(22) Day, G. M.; Cooper, T. G.; Cruz-Cabeza, A. J.; Hejczyk, K. E.; Ammon, H. L.; Boerrigter, S. X. M.; Tan, J. S.; Della Valle, R. G.; Venuti, E.; Jose, J.; Gadre, S. R.; Desiraju, G. R.; Thakur, T. S.; van Eijck, B. P.; Facelli, J. C.; Bazterra, V. E.; Ferraro, M. B.; Hofmann, D. W. M.; Neumann, M. A.; Leusen, F. J. J.; Kendrick, J.; Price, S. L.; Misquitta, A. J.; Karamertzanis, P. G.; Welch, G. W. A.; Scheraga, H. A.; Arnautova, Y. A.; Schmidt, M. U.; van de Streek, J.; Wolf, A. K.; Schweizer, B. *Acta Crystallogr.* **2009**, *B65*, 107.
(23) Oostenbrink, C.; Villa, A.; Mark, A. E.; Gunsteren, W. F. V. *J. Comput. Chem.* **2004**, *25*, 1656.
(24) Cornell, W. D.; Cieplak, P.; Bayly, C. I.; Gould, I. R.; Merz, K. M.; Ferguson, D. M.; Caldwell, J. W.; Kollman, P. A. *J. Am. Chem. Soc.* **1995**, *117*, 5179.
(25) Fronczek, F. R.; Kamelb, H. N.; Slattery, M. *Acta Crystallogr., Sect. C* **2003**, *59*, O567.
(26) Guest, M. F.; Bush, I. J.; Van Dam, H. J. J.; Sherwood, P.; Thomas, J. M. H.; Van Lenthe, J. H.; Havenith, R. W. A.; Kendrick, J. *Mol. Phys.* **2005**, *103*, 719.
(27) Kendrick, J.; Fox, M. *J. Mol. Graphics* **1991**, *9*, 182.
(28) Smith, W.; Forester, T. R. *J. Mol. Graphics* **1996**, *14*, 136.
(29) Berendsen, H. J. C.; Postma, J. P. M.; Gunsteren, W. F. v.; DiNola, A.; Haak, J. R. *J. Chem. Phys.* **1984**, *81*, 3684.
(30) Chatchawalsaisin, J.; Kendrick, J.; Tuble, S. C.; Anwar, J. *CrystEngComm* **2008**, *10*, 437.
(31) Anwar, J.; Tuble, S. C.; Kendrick, J. *J. Am. Chem. Soc.* **2007**, *129*, 2542.
(32) Beckham, G. T.; Peters, B.; Starbuck, C.; Variankaval, N.; Trout, B. L. *J. Am. Chem. Soc.* **2007**, *129*, 4714.
(33) Martoňák, R.; Laio, A.; Bernasconi, M.; Ceriani, C.; Raiteri, P.; Zipoli, F.; Parrinello, M. *Z. Kristallogr.* **2005**, *220*, 489.
(34) Jorgensen, W. L.; Tirado-Rives, J. *J. Am. Chem. Soc.* **1988**, *110*, 1657.
(35) Stone, A. J. *J. Chem. Theory Comput.* **2005**, *1*, 1128.
(36) Day, G. M.; Price, S. L. *J. Am. Chem. Soc.* **2003**, *125*, 16434.
(37) Price, S. L.; Hamad, S.; Torrisi, A.; Karamertzanis, P. G.; Leslie, M.; Catlow, C. R. A. *Mol. Simul.* **2006**, *32*, 985.

JP9052665